



Supplement of

Applying global warming levels of emergence to highlight the increasing population exposure to temperature and precipitation extremes

David Gampe et al.

Correspondence to: David Gampe (d.gampe@lmu.de)

The copyright of individual parts of the supplement might differ from the article licence.

Contents of this file

Figures S1 to S15

Introduction

This document contains the supporting information for the main study presented as supplementary figures. All presented figures are referenced in the text and considered relevant to support the main findings and highlight dependencies on different approaches, thresholds or remapping sequencing.

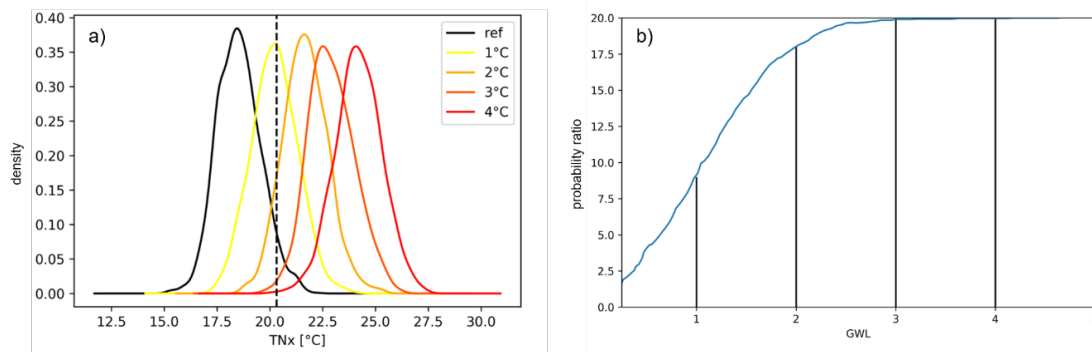


Figure S1. Schematic overview of the calculation of extremes and the related probability ratio (PR). a) shows the probability density functions of TNx at a single grid point for the reference period (1850-1900; black) and selected Global Warming Levels (GWLs 1-4°C; colored). The graph illustrates the shift of the distribution towards higher values with increasing GWLs. The dotted line indicates the given threshold (95th percentile of the reference distribution for PR; analogous for GWLoE). b) illustrates the concept of GWL-dependent probability ratio increases. The curve slope is largest for GWLs between 1 and 2 °C and flattens out for GWLs between 2 and 3 °C. This saturation relates to the fact that each year will show an exceedance of present extreme thresholds (95th percentile; see a) from 2.5°C GWL on.

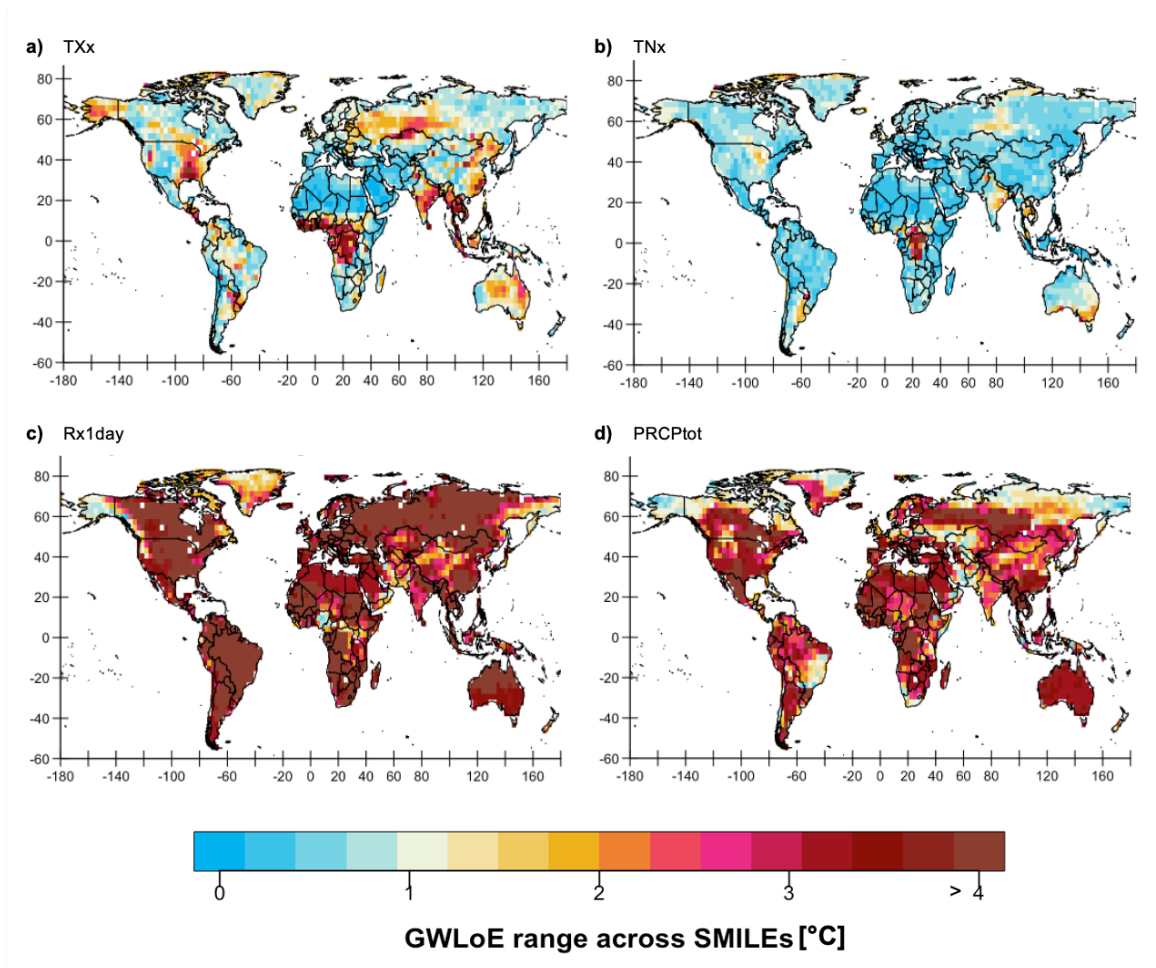


Figure S2. Inter-model range of Global Warming Level of Emergence (GWLoE) for the selected indices. The range was calculated as difference between the minimum and maximum GWLoE across the five bootstrapped SMILEs (based on the mean across 1000 GWLoE samples for each SMILE) for TXx (a), TNx (b), Rx1day (c) and PRCPtot (d).

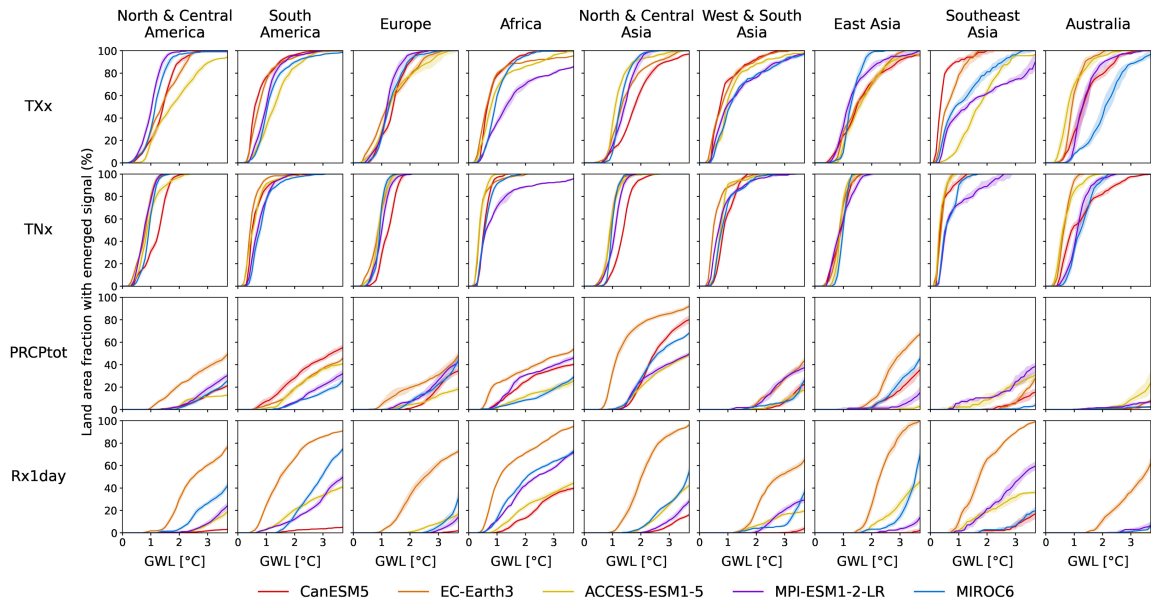


Figure S3. Fraction of the land area exposed to emerged climate indices in dependence of the Global Warming Level (GWL) to changes in TXx, TNx, PRCPtot and Rx1day stratified across regions. Different colors represent the five SMILEs and shading the 95% confidence interval estimated by bootstrapping (see methods).

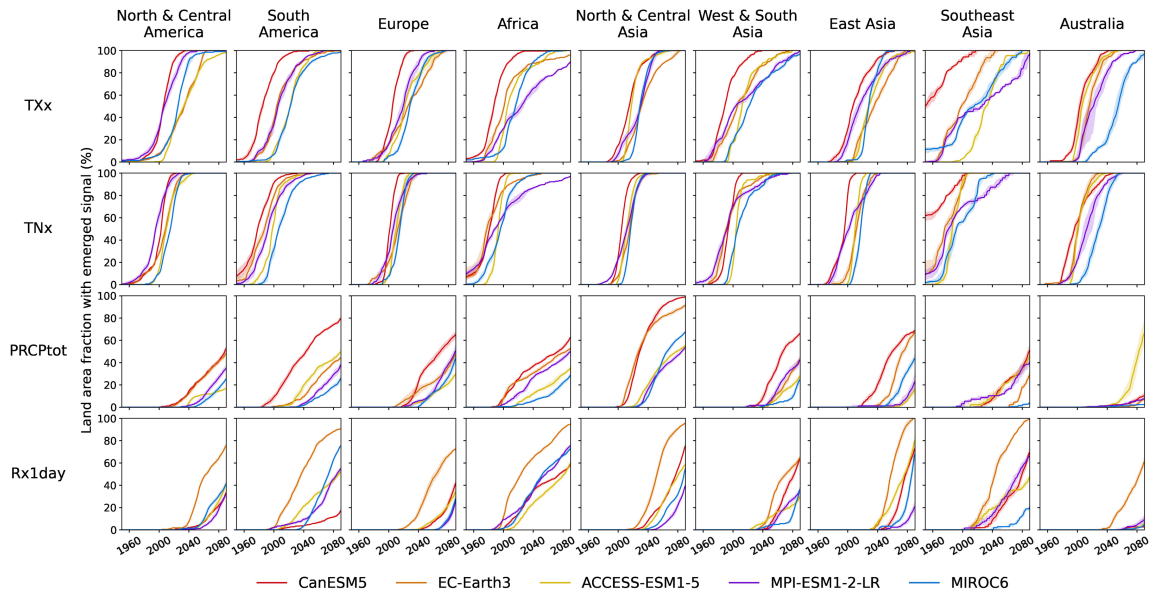


Figure S4. Fraction of the land area exposed to emerged climate indices in dependence of the time (Time of Emergence) to changes in TXx, TNx, PRCPtot and Rx1day stratified across regions. Different colors represent the five SMILEs and shading the 95% confidence interval estimated by bootstrapping (see methods).

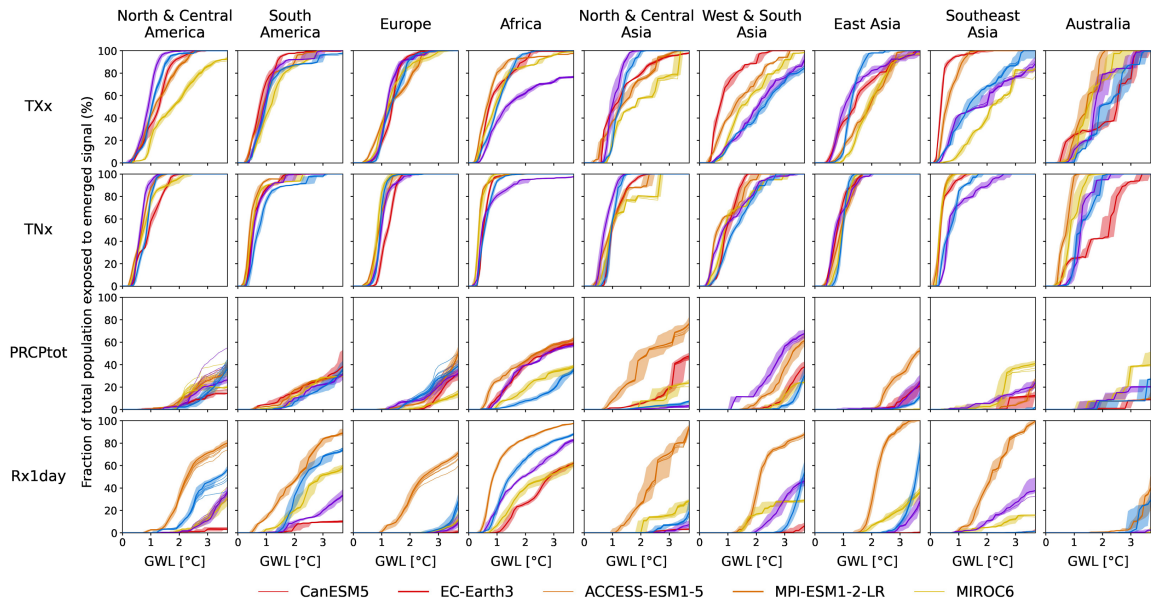


Figure S5. Fraction of the total population exposed to emerged climate indices in dependence of the Global Warming Level (GWL) to changes in TXx, TNx, PRCPot and Rx1day stratified across regions. Different colors represent the five SMILEs and shading represents the 95% confidence interval estimated by bootstrapping (see methods). The different lines indicate the exposure according to different population scenarios, with the thick line corresponding to a population development according to SSP5 and the thin lines to population developments according to SSP1-SSP4.

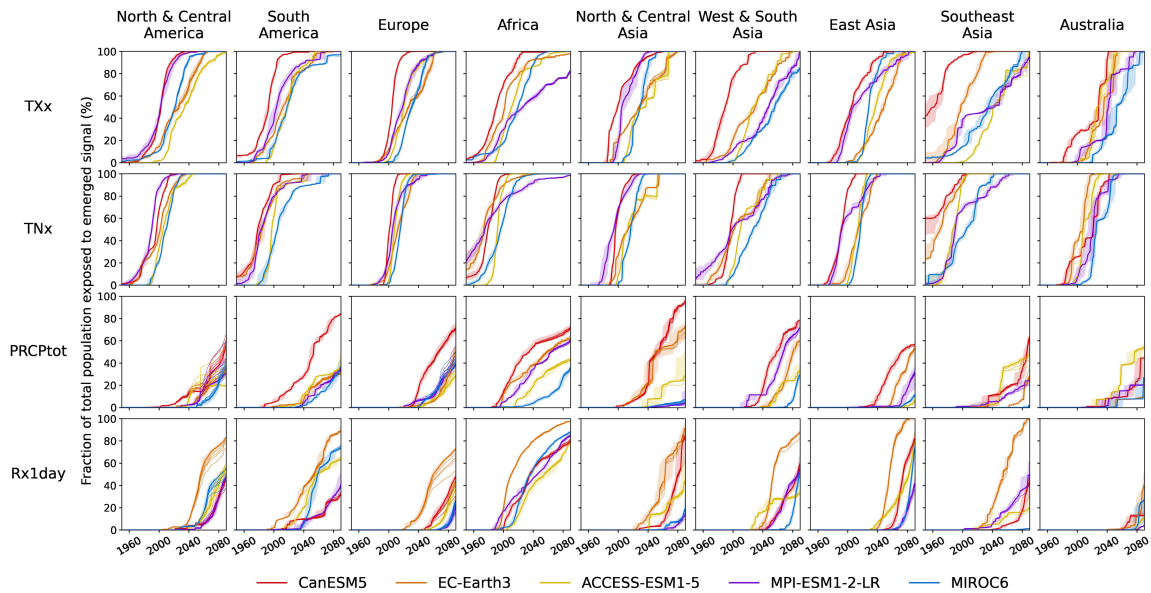


Figure S6. As in Figure S5 but as function of time (Time of Emergence).

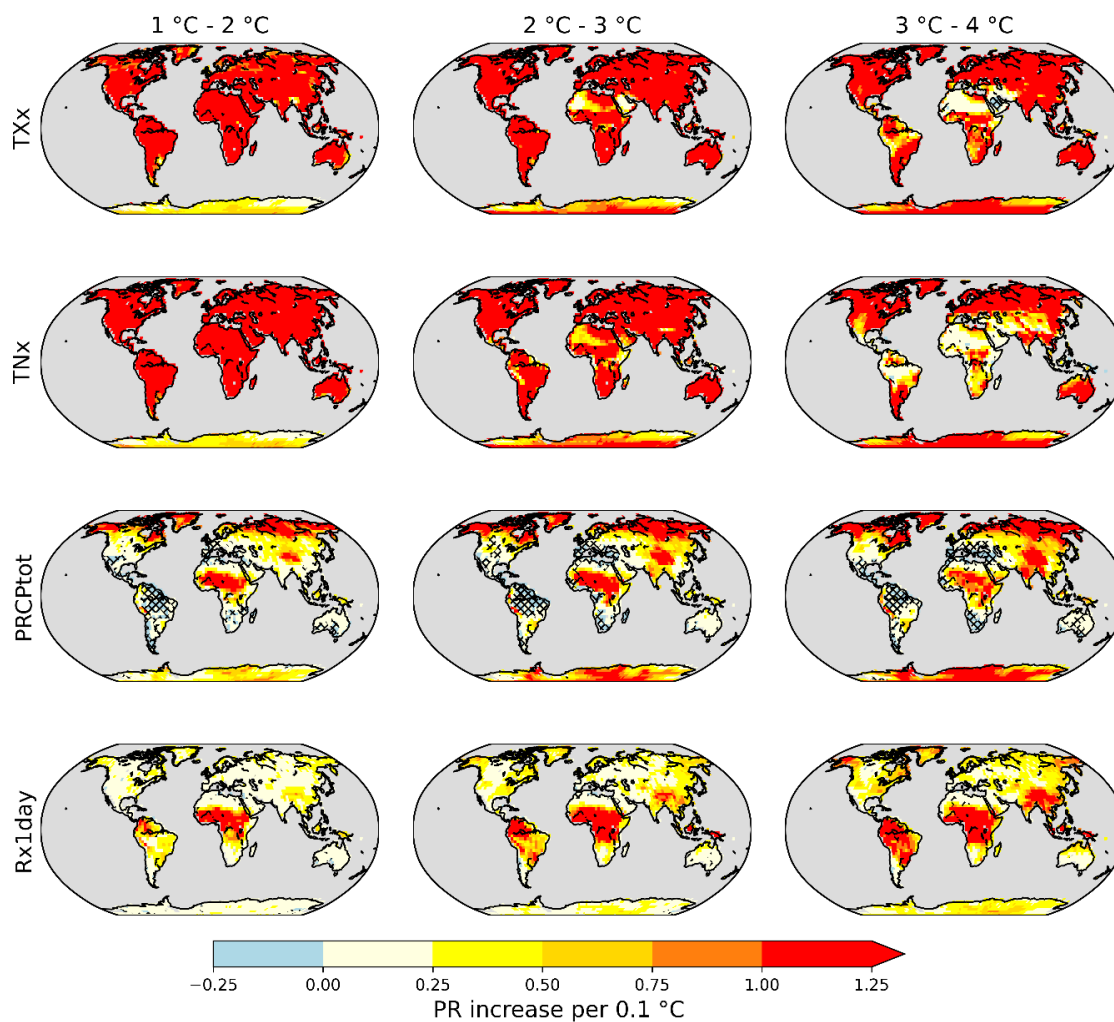


Figure S7. Average increase in probability ratio for selected warming level ranges for the considered indices at the 99th percentile threshold. The changes are presented as increases (brown) or decreases (purple) per 0.1° C warming (calculated with respect to 1850-1900 conditions). The probability ratio (PR) refers to the hazard imposed by the occurrence of extremes extreme (>99th percentile during the pre-industrial period; calculated across all members per ensemble over 20-year periods; see Methods for details). Hatched areas depict regions where more than 1 SMILE disagree in sign of the PR.

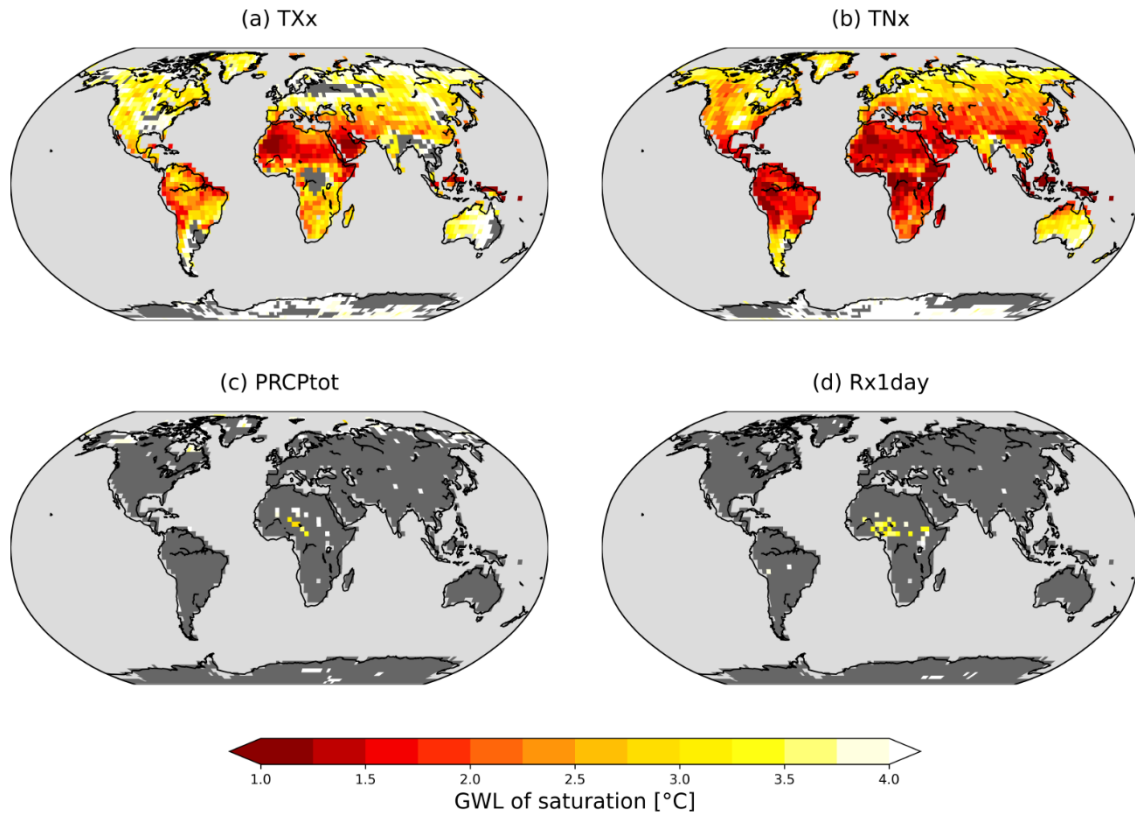


Figure S8. Global Warming Level (GWL) of saturation for moderate events (i.e., exceeding 50th pre-industrial percentiles) of the considered indices (ensemble median across all SMILEs is shown where at least 4 out of 5 SMILEs show saturation values). Here, saturation is defined as the GWL where the maximum number of events per 20-year period (20 out of 20 years) is reached, i.e., each year marks a moderate event relative to pre-industrial conditions.

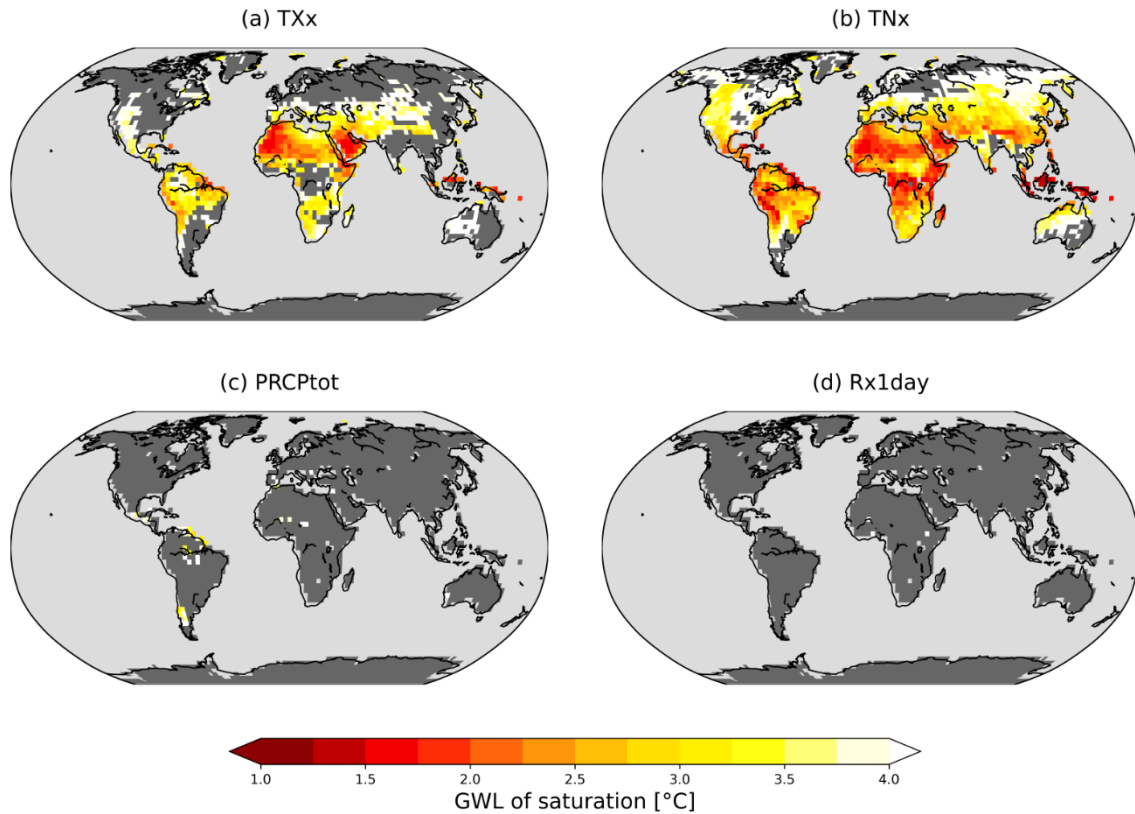


Figure S9. Global Warming Level (GWL) of saturation for extreme events (i.e., exceeding 90th pre-industrial percentiles) of the considered indices (ensemble median across all SMILEs is shown where at least 4 out of 5 SMILEs show saturation values). Here, saturation is defined as the GWL where the maximum number of events per 20-year period (20 out of 20 years) is reached, i.e., each year marks an extreme relative to pre-industrial conditions.

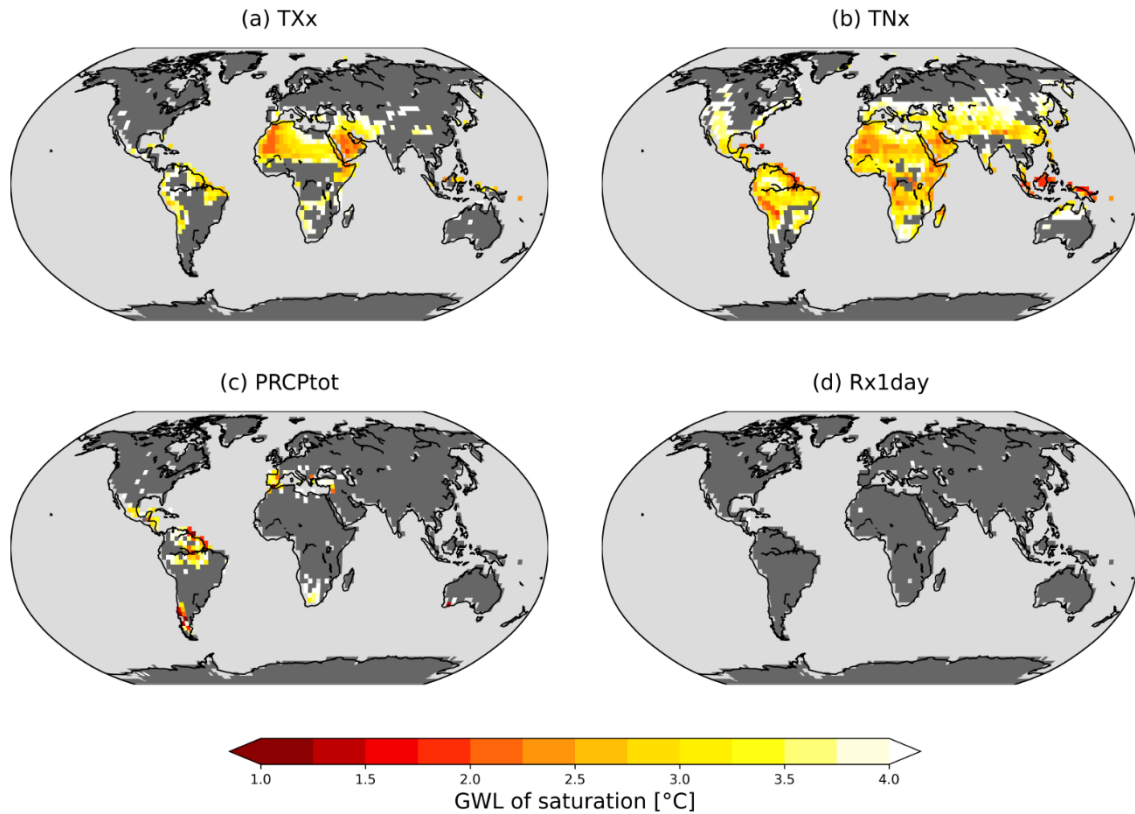


Figure S10. Global Warming Level (GWL) of saturation for extreme events (i.e., exceeding 99th pre-industrial percentiles) of the considered indices (ensemble median across all SMILEs is shown where at least 4 out of 5 SMILEs show saturation values). Here, saturation is defined as the GWL where the maximum number of events per 20-year period (20 out of 20 years) is reached, i.e., each year marks an extreme relative to pre-industrial conditions.

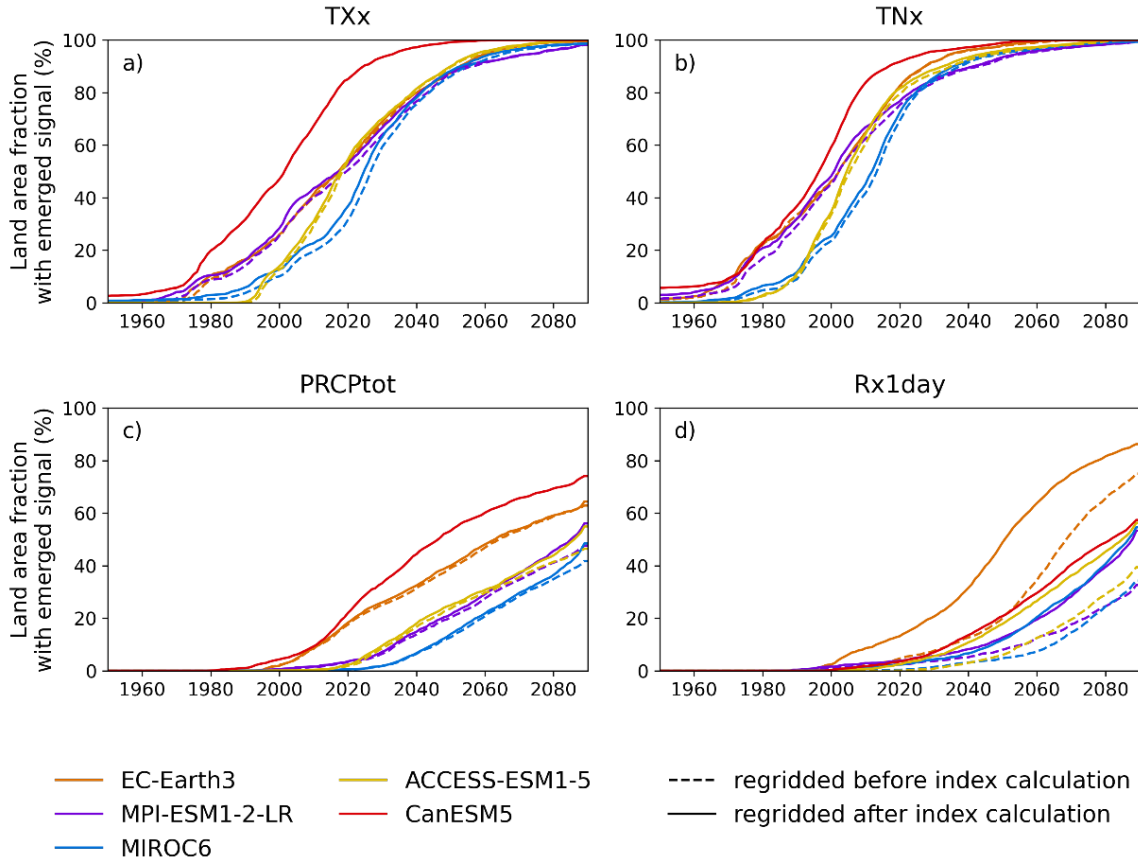


Figure S11. Fraction of the land area exposed to emerged climate indicators in dependence of time (ToE). The panels show the related land area fraction with respect to the emergence of TXx (a), TNx (b), PRCPtot (c) and Rx1day (d) for two different spatial aggregation approaches for a subset of each ensemble. Solid lines are based on the calculation of the corresponding index at the native resolution (see Tab. 1) which were then aggregated to the CanESM5 grid ($2.8^{\circ} \times 2.8^{\circ}$) as applied throughout the study (*local extremes*). For the dashed lines, the corresponding temperature and precipitation fields were aggregated to the coarser resolution *before* the index calculation (*harmonized approach*).

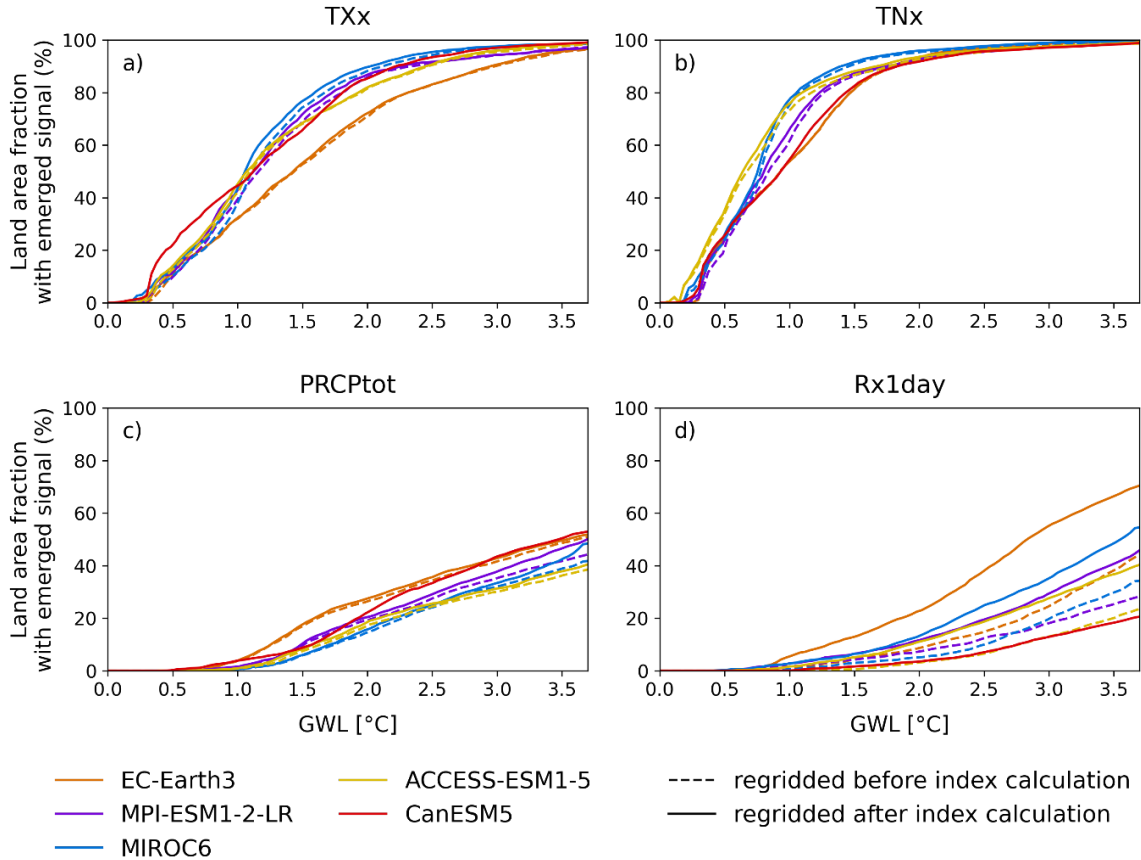


Figure S12. Fraction of the land area exposed to emerged climate indicators in dependence of the Global Warming Level (GWL; GWLoE). The panels show the related land area fraction with respect to the emergence of TXx (a), TNx (b), PRCPtot (c) and Rx1day (d) for two different spatial aggregation approaches for each ensemble. Solid lines are based on the calculation of the corresponding index at the native resolution (see Tab. 1) which were then aggregated to the CanESM5 grid (2.8°x2.8°) as applied throughout the study (*local extremes*). For the dashed lines, the corresponding temperature and precipitation fields were aggregated to the coarser resolution *before* the index calculation (*harmonized approach*).

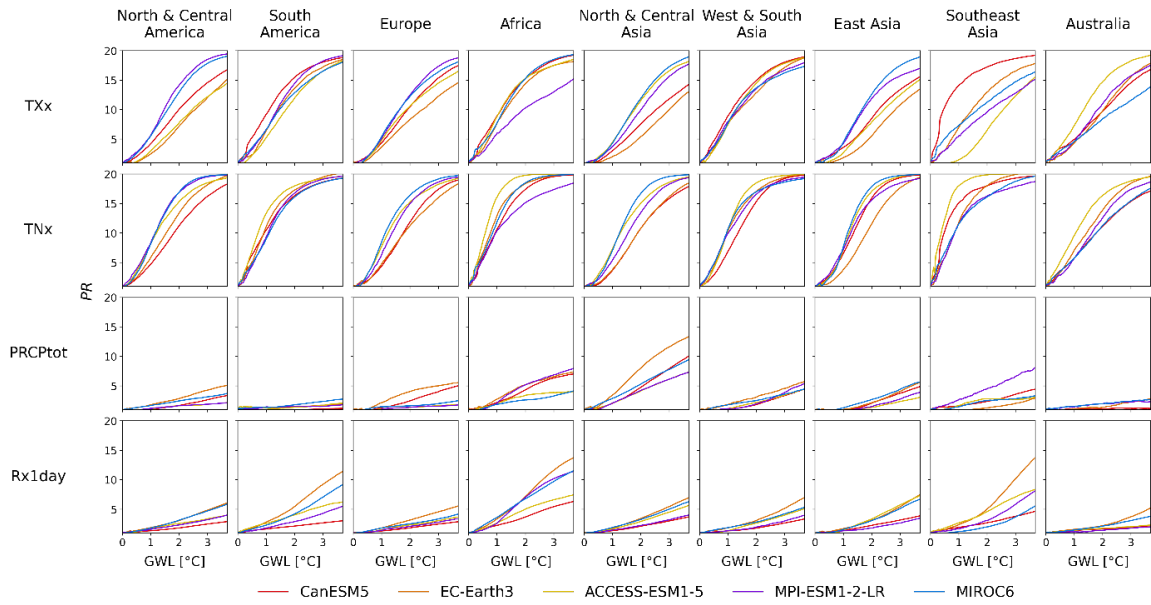


Figure S13. Probability ratio (PR) in dependence of Global Warming Level (GWL) for the considered indices TXx, TNx, PRCPtot and Rx1day over selected regions. Probability ratios are presented for each SMILE and calculated with respect to pre-industrial (1850-1900) climate conditions.

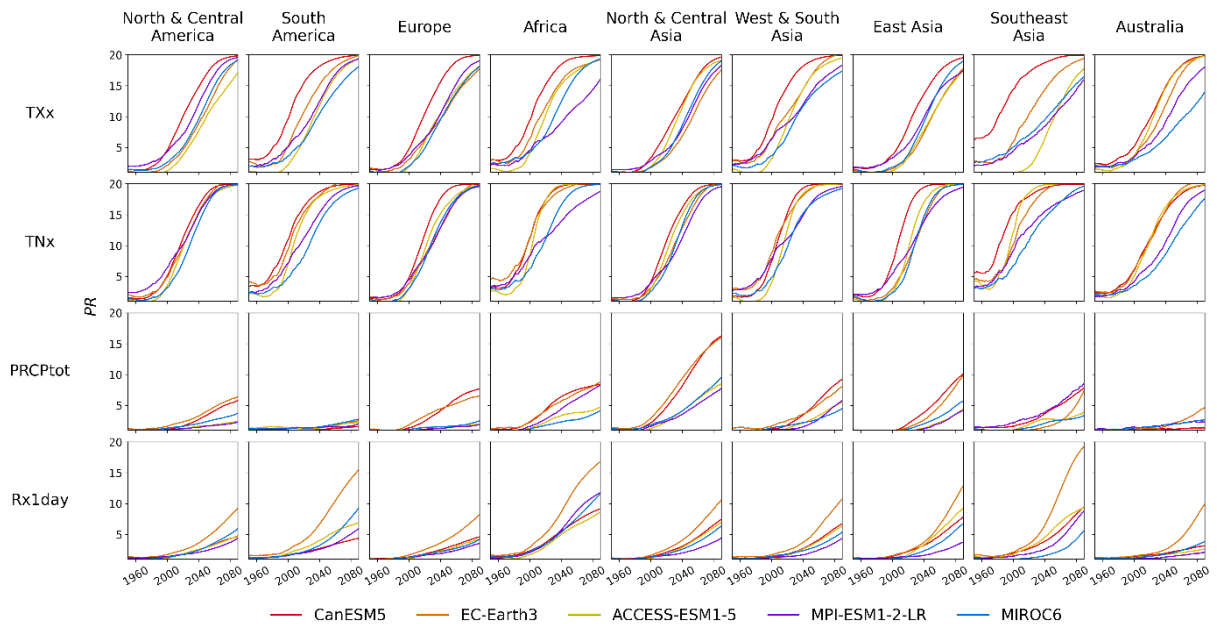


Figure S14. Probability ratio (PR) in dependence of time for the considered indices TXx, TNx, PRCPtot and Rx1day over selected regions. Probability ratios are presented for each SMILE and calculated with respect to pre-industrial (1850-1900) climate conditions.

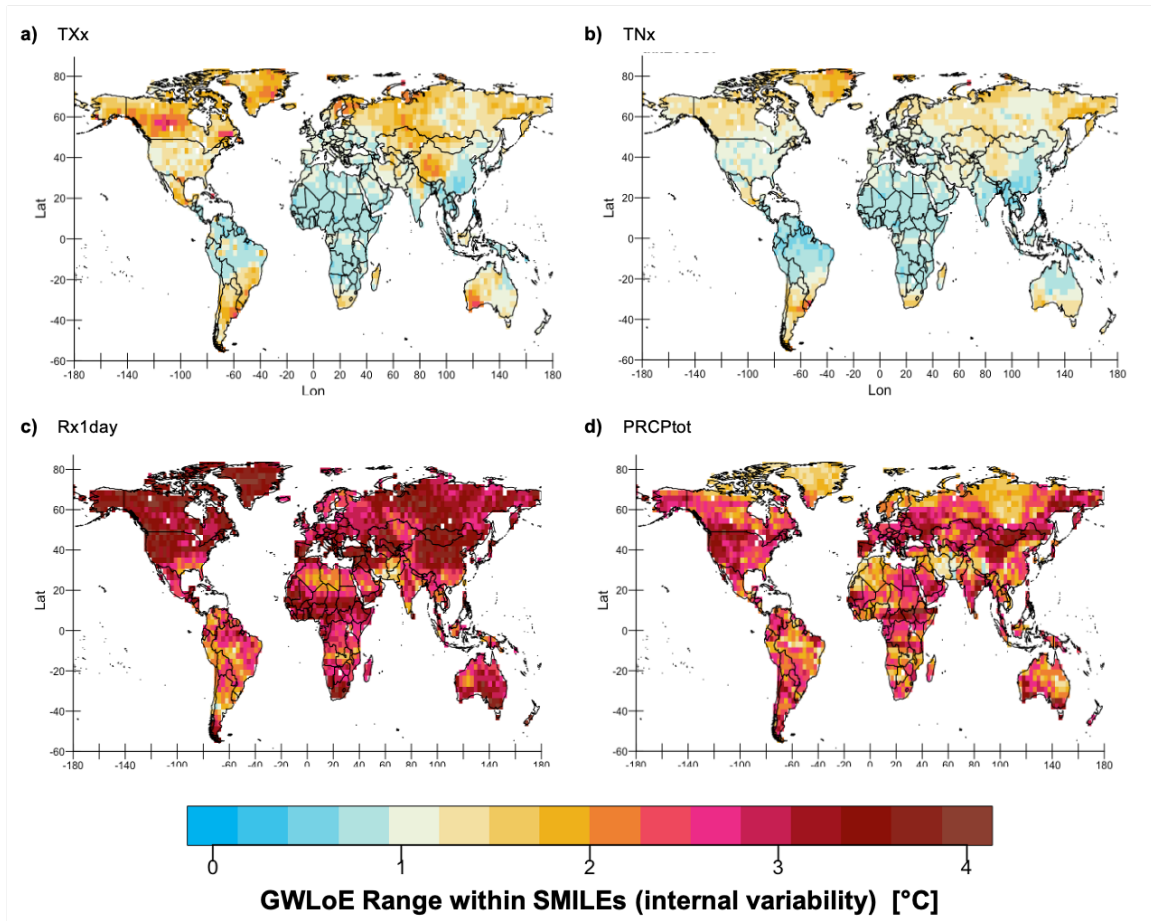


Figure S15. Range of Global Warming Level of Emergence (GWLoE) across the members of each SMILE for the indices TXx (a), TNx (b), Rx1day (c) and PRCPtot (d). The average range reflects internal variability and was calculated as mean across the five SMILEs (based on the min-max range of GWLoE across the members of each SMILE).